A Multiple-Process Equilibrium Analysis of Silica Gel and HZSM-5

Russell S. Drago,*,† Charles Edwin Webster,* and J. Michael McGilvray

Contribution from the Center for Catalysis, Department of Chemistry, University of Florida, Gainesville, Florida 32611

Received July 9, 1997[⊗]

Abstract: Adsorption isotherms are reported for HZSM-5 and silica gel using a series of gas adsorptives at several temperatures above their critical temperature. The data are analyzed with a new multiple equilibria adsorption model producing equilibrium constants (K_i), capacities (n_i), and enthalpies ($-\Delta H_i$) for each of the processes. Unlike the amorphous adsorbents studied earlier, which contain a distribution of pore sizes, zeolitic materials have uniform pore dimensions. This uniformity provides a test of our interpretation of the number of processes required in the isotherm fits of the multiple equilibrium analysis, MEA. As expected from the two pores in the structure of HZSM-5, most adsorbates require two processes ($K_{1,ads}$ and $K_{2,ads}$) to fit the adsorption isotherms. HZSM-5 is compared to amorphous carbonaceous adsorbents, revealing fundamental differences in their behavior. Small cylindrical channels in HZSM-5 lead to an unfavorable entropic contribution from restrictions imposed by adsorptive packing and interactions with the channel walls. The pores of the carbons studied (Drago, R. S.; Kassel, W. S.; Burns, D. S.; McGilvray, J. M.; Lafrenz, T. J.; Showalter, S. K. *J. Phys. Chem. B* **1997**, *101*, 7548−7555) are slit-shaped, leading to less restriction and larger equilibrium constants. For several adsorbates, the greater enthalpic interactions in the small HZSM-5 pores are accompanied by lower equilibrium constants than in the larger pores because of unfavorable entropic contributions. Finally, the larger total micropore volumes of the carbons studied for these adsorptives (Drago, R. S.; Kassel, W. S.; Burns, D. S.; McGilvray, J. M.; Lafrenz, T. J.; Showalter, S. K. *J. Phys. Chem. B* **1997**, *101*, 7548−7555) result in increased capacity compared to HZSM-5. The process capacities from MEA (mol g^{-1}) are converted to pore volumes using the molar volume. Surface areas are calculated from molecular areas of the adsorbates. Pore volumes and surface areas calculated from the process capacities are compared to those from conventional N_2 porosimetry and are shown to provide a more detailed and more accurate assessment of areas and volumes. These results show that MEA has the potential of becoming a standard characterization method for microporous solids that will lead to an increased understanding of their behavior in gas adsorption and catalysis.

Introduction

Equation 1 describes the physisorption of a gas, $A_{(g)}$, by a solid surface, $S_{(s)}$. An adsorption equilibrium constant, K, for

$$S_{(s)} + A_{(g)} \Leftrightarrow SA_{(s)} \tag{1}$$

eq 1 can be written and rearranged to give eq 2,[1,2] where n is

$$[SA]_s = \frac{nK[P]}{1 + K[P]} \tag{2}$$

the capacity for adsorption, $[SA]_s$ is the total amount of A adsorbed per gram of solid, and P is the equilibrium pressure, atm, of gaseous A in equilibrium with the solid. The novel feature of our approach is the treatment of nonspecific adsorption by this distribution type of equilibrium constant (like a distribution coefficient) that refers to a process and not to a specific, isolated binding site on a planar surface. Thus, though eq 2 is similar in form to the Langmuir equation, the MEA derivation, with n defined as a process capacity, leads to a conceptually different model and eliminates the assumptions required[2] to apply the Langmuir model to binding at a solid site. The n of eq 2 provides the process capacity of an equilibrium process that involves adsorbate in *similar* size pores undergoing *similar* energies of interaction with the solid and neighbor adsorbate molecules.

In the first two papers of this series,[3,4] it has been shown that, for porous carbonaceous materials, a simple one-process model does not adequately describe adsorption isotherms for gases above their critical temperature and up to 1 atm of external pressure. Several equilibria like that in eq 1 may be involved, and summation of i expressions like eq 2, to accommodate i multiple adsorption processes, leads to eq 3. Each of the i

$$[SA]_s = \sum_i \frac{n_i K_i[P]}{1 + K_i[P]} \tag{3}$$

adsorption processes is treated by a separate equilibrium constant, and the total adsorption isotherm is the sum of the individual isotherms for each i process.

A novel feature of this multiple-process, equilibrium analysis, MEA, is the accurate definition of the K and n values by

* Address correspondence to C. E. Webster. Phone: (352) 392-5263. Fax: (352) 392-4658.

† Deceased, Dec. 5, 1997.

⊗ Abstract published in *Advance ACS Abstracts,* December 15, 1997.

(1) Gregg, S. J.; Sing, K. S. W. *Adsorption, Surface Area, and Porosity*; Academic Press: London, 1967.

(2) Adamson, A. W. *Physical Chemistry of Surfaces*, 5th ed.; John Wiley & Sons, Inc.: New York, 1990.

(3) Drago, R. S.; Burns, D. S.; Lafrenz, T. J. *J. Phys. Chem.* **1996**, *100*, 1718−1724.

(4) (a)Drago, R. S.; Kassel, W. S.; Burns, D. S.; McGilvray, J. M.; Lafrenz, T. J; Showalter, S. K. *J. Phys. Chem. B* **1997**, *101*, 7548−7555. (b)Kassel, W. S.; Drago, R. S. *Microporous Mater.* In press.

S0002-7863(97)02466-9 CCC: $15.00
Published on Web 01/08/1998

measuring adsorption isotherms at several temperatures. The values for $n_{i,ads}$, like solid densities, are essentially temperature independent; therefore, new temperatures introduce as unknowns only the new $K_{i,ads}$ for each process. Adsorption measurements at several temperatures not only provide meaningful equilibrium adsorption K and n values, by a better definition of the minimum in a least-squares data fit, but also provide enthalpies of adsorption for each process via the van't Hoff equation. In contrast to the BET model, the MEA model fits the total adsorption isotherm at each temperature and provides equilibrium constants, capacities, and enthalpies for each adsorption process. The capacity of the solid for the various processes, $n_{i,ads}$, mol g^{-1}, can be converted to accessible pore volumes for the different processes using the adsorbate's molar volume, and for monolayer coverage, the corresponding surface areas utilized can be determined from adsorbate molecular areas.

The different equilibria correspond to adsorption in pores of different sizes. In the absence of donor−acceptor interactions, the smallest accessible pores are expected[5] to have the more negative enthalpy and the largest pores the less negative enthalpy. In an amorphous solid containing a distribution of pore sizes, like carbon, the sizes of the pores utilized for the different processes will vary with the sorptive size. Studying a solid with regular, known pore dimensions will provide a test of the MEA by checking the relation between the structure and the number of processes needed to fit the isotherm. Such a porous, crystalline solid is provided by the aluminosilicate HZSM-5 which consists of straight channels and intersecting perpendicular zigzag channels.[6−9] The dimensions of the elliptical straight channel are reported as 5.4 × 5.6 Å and those of the intersecting, sinusoidal channel as 5.1 × 5.4 Å.[10] June *et al.*[11] calculate that the intersections of the zigzag and straight channels of silicalite will lead to roughly 9.0 Å voids. The different channel dimensions should lead to at least two different affinity adsorption processes and allow us to determine if MEA can distinguish them.

There are additional advantages to studying HZSM-5. Though applications of zeolites[12,13] as shape selective catalysts and adsorbents are related to zeolite porosity, determination of the pore volume is not straightforward and remains uncertain. Saito and Foley[14] reported adsorption isotherms for nitrogen and argon at 77 K on high alumina content HZSM-5 samples (Si/Al = 23). Using the Horvath−Kawazoe, H−K, model to calculate the pore size distribution, an observed single transition in the isotherm resulted in a calculated pore diameter of 5.5 Å. At higher Si/Al ratios (70 and >400), the 5.5 Å pore transition is also found, but in addition, a second transition is observed in the isotherm corresponding to a calculated pore diameter of 7.7 Å. This larger pore diameter was reported to be a nonexistent artifact. The defined porosity, H−K complications and extensive literature on theoretical modeling make the study of zeolites an important challenge for the development of our model.

For most adsorbates that do not undergo specific interactions, the extension of MEA to HZSM-5 requires two processes. The K and n values for various size probe molecules provide added insight regarding the influence of pore dimensions on adsorbent affinity and capacity. The trends observed in the MEA parameters for different adsorptives show patterns expected for an adsorbent with defined porosity and in so doing support our claim that MEA is not meaningless data fitting with multiple parameters. Instead, the resulting thermodynamic data, pore volumes, and surface areas for the different adsorptives provide a characterization of adsorption by solids that is unique in the detail provided. The MEA characterization of microporous HZSM-5 and Fisher silica gel, materials of similar composition, affords a dramatic comparison of the influence of porosity on the adsorption process.

Experimental Section

Gases. The gases CH_4, CO, C_2H_6, C_3H_8, and DME (99.99%) were purchased from Matheson Gas. N_2 (99.99%) was purchased from Liquid Air, Inc. Sulfur hexafluoride (SF_6) was purchased from Aldrich Chemical. All gases were used as received without further purification.

Solid Characterization. Silica gel was purchased from Fisher Scientific (lot no. 934403), and HZSM-5 (Si/Al = 53) was donated by PQ Corp. Carbon and nitrogen analyses were performed by the University of Florida elemental analysis laboratory. The HZSM-5 contained 0.61% carbon which corresponds to 0.05 mmol of template or 0.5 mmol of carbon from residual alkoxide. Nitrogen at 0.25% is within the 0.4% limit of the analysis. Silica gel gave no carbon or nitrogen. In view of the small amount of impurities, the solids, as received, were degassed under vacuum ($<10^{-4}$ Torr) for 8 h at 200 °C and then studied. The infrared spectrum of HZSM-5 subjected to these drying conditions showed no bands from water or ammonium ions.

For comparative purposes, surface area and pore volume data were measured with N_2 adsorption at 77 K using a Micromeretics ASAP 2000 gas analyzer. Surface areas are reported using a five-point BET calculation.[15] Micropore volume was determined using the Harkins−Jura *t*-plot model with thickness parameters from 5.0 to 10.0 Å.[16] Macro- and mesopore volumes were calculated using the Barrett−Joyner−Halenda (BJH) desorption curve.[17]

Adsorption Measurements. Gaseous uptake measurements on porous silica gel and HZSM-5 were performed on a Micromeretics ASAP 2000 instrument with chemisorption/physisorption software employing a 47-point pressure table ranging from 0.1 to 760 Torr on samples degassed for 8 h. The system was considered to be at equilibrium when the pressure change was less than 1% of the selected pressure point in a 10 s equilibration time interval. Pressure tolerances were 1% with the 10 Torr transducer and 1 mmHg with the 1000 Torr transducer. Low-temperature baths, consisting of a solvent/liquid nitrogen mixture, were required to collect isotherms at low temperatures.[18] Studies involving condensable gases (ethane, propane, DME, and SF_6) required elevated temperatures that were obtained with insulated heating mantles which maintained the temperature to within ±1 °C. All measurements are carried out at or above the critical temperatures.

Equilibrium Analysis. The measured isotherms were analyzed using eq 3 by a procedure that was previously described.[3,4] In using this equation, the minimum number of processes required to obtain a good data fit are utilized. A detailed explanation of the criteria for selecting the correct number of processes is reported.[4b] One starts the

(5) Everett, D. H; Powl, J. C. *J. Chem. Soc., Faraday Trans. 1* **1976**, *72*, 619.
(6) Breck, D. W. *Zeolite Molecular Sieves*; John Wiley & Sons: New York, 1974.
(7) Chen, N. Y.; Degnan, T. F.; Smith, C. M. *Molecular Transport and Reaction in Zeolites*; VCH Publishers: New York, 1994.
(8) Dyer, A. *An Introduction to Zeolite Molecular Sieves*; John Wiley & Sons: New York, 1988.
(9) Jansen, J. C., Stocker, M., Karge, H. G., Weitkamp, J., Eds. *Advanced Zeolite Science and Applications*; Elsevier: Amsterdam, 1994; Vol. 85.
(10) Olson, D. H.; Kokotailo, G. T.; Lawton, S. L.; Meier, W. M. *J. Phys. Chem.* **1981**, *85*, 2238.
(11) June, R. L.; Bell, A. T.; Theodoro, D. N. *J. Phys. Chem.* **1990**, *94*, 1508−1516.
(12) Bhatia, S. *Zeolite Catalysis: Principles and Applications*; CRC Press: Boca Raton, FL, 1990.
(13) Iler, R. K. *The Chemistry of Silica*; John Wiley & Sons: New York, 1979.
(14) Saito, A.; Foley, H. C. *Microporous Mater.* **1995**, *3*, 543−556.
(15) Brunauer, S.; Emmett, P. H.; Teller, E. *J. Am. Chem. Soc.* **1938**, *60*, 309.
(16) Harkins, W. D.; Jura, G. *J. Am. Chem. Soc.* **1944**, *66*, 1366.
(17) Barrett, E. P.; Joyner, L. G.; Halenda, P. P. *J. Am. Chem Soc.* **1951**, *73*, 373.
(18) Gordon, A. J.; Ford, R. A. *The Chemist's Companion*; John Wiley and Sons: New York, 1972; p 451.

Table 1. Physical Properties of Adsorbents

	Fisher SG	PQ-ZSM5
BET surface area[a] (m^2/g)	508	402
pore volume (mL/g)		
micropore[b]	0.02	0.14
mesopore[c]	0.33	0.17
macropore[c]		

[a] Surface area and pore volume data are from N_2 porosimetry at 77 K. [b] Micropore volumes calculated from the Harkins−Jura *t*-plot model. [c] Meso- and macropore volumes calculated from Barrett−Joyner−Halenda (BJH) desorption data.

MEA by taking each individual data set and graphing it as P_{atm}/moles adsorbed vs P_{atm}. For one adsorption process, eq 3 reduces to a straight line with the slope of the line equal to $1/n$ and the intercept equal to $1/nK$. The graphs of the individual data sets are curved and not linear, indicating multiple processes. Linear regions can be found in the curved plot and a linear regression performed on these regions to obtain a rough estimate of n and K for the processes. The data sets at different temperatures introduce new $K_{i,ads}$ values for each process, but the $n_{i,ads}$ values from these plots remain fairly constant for the different temperature data sets of a particular probe. The n and K values obtained for each process from the linear portion of the isotherm are then used as seed values in a modified least-squares minimization, simplex fitting program which has been designed to simultaneously fit the combined temperature sets of adsorption data for a particular adsorptive. Low-temperature data provide the most accurate n and $K_{i,ads}$ values for process 2, whereas higher temperatures provide more accurate values for process 1. This is reflected by examining the data fits where the process 1 capacity at low temperature is filled within the first two or three pressure measurements, providing little information to calculate the process 1 parameters. However, most of the isotherm at low temperature corresponds to process 2, leading to an accurate determination of these parameters. Experiments at higher temperature will not adsorb as much of the gas at or below 1 atm, leading to a more extensive data set for determination of the process 1 parameters.

Results and Discussion

Silica gel (amorphous) and HZSM-5 (crystalline) have similar compositions but different porosities. Fisher silica gel is reported to consist of a distribution of mainly mesopores. X-ray data indicate that the channels and voids from channel intersections in HZSM-5 have fixed dimensions and are microporous. In contrast to these conclusions from X-ray data, results from standard N_2 porosimetry would lead to the incorrect conclusion that our sample of HZSM-5 contains comparable volumes of micro- and mesopores (Table 1). The BET surface area of 402 $m^2\ g^{-1}$ is also uncertain, for it is reported[1] that shortcomings of the BET model can lead to prediction of too large of a surface area for microporous solids. Thus, MEA of HZSM-5 using nonpolar adsorbates of varying dimensions and shapes above their critical temperatures not only will provide a test of the significance of the MEA parameters but also can offer an alternative to BET for surface areas and to the H−J *t*-plot and BJH for determining pore volumes of porous solids.

Adsorption Isotherms. Experimental adsorption isotherms for HZSM-5 (Si/Al = 53) are given by the points in Figures 1 and 2, and sample data fits are illustrated by the solid lines. The physical properties of the adsorbates used are summarized in Table 2. The temperature dependent $K_{i,ads}$ values for all systems studied are listed in Table 3. The calculated $n_{i,ads}$ values are listed in Table 4. Measurements at several temperatures for most gases show that in the absence of donor−acceptor interactions two processes are able to fit the adsorption data to experimental accuracy. Criteria have been reported[4b] for determining the number of processes required. The existence

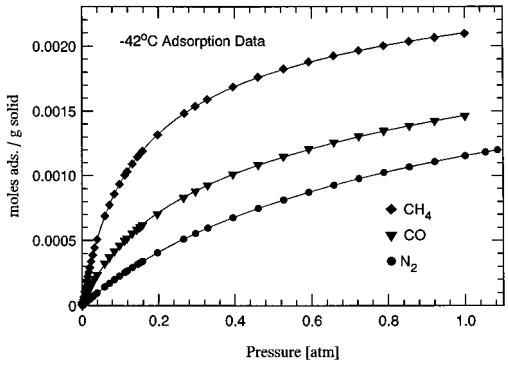

Figure 1. Adsorption isotherms for the small molecules at −42 °C on HZSM-5. The symbols are the experimental data points, and the solid lines are the calculated isotherms from the MEA n and K values.

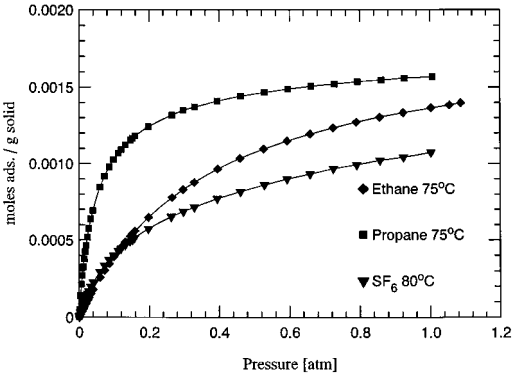

Figure 2. Adsorption isotherms for the larger molecules on HZSM-5. The symbols are the experimental data points, and the solid lines are the calculated isotherms using the n and K values from the MEA.

of at least two processes is expected because two different channels exist, one straight and one zigzag, with different dimensions.

The temperature dependence of $K_{i,ads}$ gives the enthalpies ($-\Delta H_{i,ads}$) and entropies ($-\Delta S_{i,ads}$) for the processes via the van't Hoff equation. These results are summarized in Table 5, and the ln $K_{1,ads}$ vs $1/T(K)$ plots for HZSM-5 are shown in Figure 3. The linearity of these and reported plots,[4] as well as resulting enthalpies whose magnitudes are those expected for physisorption processes,[19] support our contention that meaningful thermodynamic parameters result from the model.

Summary of the HZSM-5 Thermodynamic Data. The process designation[3,4] gives the order of pore filling and assigns the lowest number to the process with the largest equilibrium constant. In earlier studies of amorphous carbons, the lower numbered processes also were more exothermic, corresponding to adsorption in the smaller pores of the solid. Process 1 corresponded to pores that are near the size of the gas adsorptive and had the greatest enthalpy of interaction ($-\Delta H_1$) because the adsorbed molecule interacts with both walls of the slit-shaped carbon pores. Process 2 pores are 1.2−1.4 times as large, and process 3 pores are above 1.4 and below 2 times the size of the gaseous adsorbate. Decreased interaction with the opposite wall accompanies increasing pore size. Comparison of the diameters of the probes (Table 2) suggests that the small channel diameter of HZSM-5 is large enough to accommodate SF_6 and 1.5 times larger than the diameter of the smaller gas molecules studied. Thus, in contrast to carbon where the adsorbate selects those pores with comparable dimensions for process 1 from the

(19) White, M. *Heterogeneous Catalysis*; Prentice Hall: Englewood Cliffs, NJ, 1990.

Table 2. Summary of Gases and Physical Properties[a]

probe gas	MW (g/mol)	polarizability[b] (Å^3)	dipole moment (D)[c]	molar volume[d] (mL/mol)	critical temp (°C)	normal boiling point (°C)	ΔH_v (kcal/mol)	ΔS_v (cal/(mol·K))	van der Waals const (*a*)	molecular area[d] (Å^2)	molecular radius[d] (Å)
N_2	28.01	1.74	0	25.02	−146.9	−195.8	1.332	17.22	1.390	15.27[e]	2.149
CO	28.01	1.95	0.13	28.28	−140.2	−191.5	1.443	17.67	1.485	15.77[e]	2.238
CH_4	16.04	2.59	0	29.74	−82.60	−161.5	1.96	17.5	2.253	16.26[e]	2.276
C_2H_6	30.07	4.47	0	47.21	32.3	−88.65[b]	3.51	19.0	5.489	24.01[e]	2.655
C_3H_8	44.10	6.29	0.084	64.53	96.7	−42.1	4.54	19.6	8.664	28.27[e]	2.946
SF_6	146.05	6.54	0	77.04	45.55	-63.8_{sub}	4.08	19.5	7.365[f]	31.17[e]	3.126
DME	46.07	5.16	1.3	56.36	127	−24.9	5.13	20.7	8.073	26.16[e]	2.816

[a] *Lange's Handbook of Chemistry*, 13th ed.; McGraw-Hill: New York, 1985. All data are from this source unless otherwise specified. [b] *Handbook of Chemistry and Physics*, 71st ed.; CRC Press: Boca Raton, FL, 1991. [c] McClellan, A. L. *Tables of Experimental Dipole Moments*; W. H. Freeman and Co.: San Francisco, 1963. [d] Due to contradictions in the literature values, molar volumes, surface areas, and molecular radii of the adsorbates are calculated using ZINDO.[22] [e] N_2, CO, CH_4, and C_2H_6, *z*-axis parallel to plane. C_3H_8 and DME, *z*-axis perpendicular to plane. SF_6 and F face on plane. Other orientations are possible: for CO, specific interaction, *z* perpendicular to plane, 11.31 Å^2; for CH_4, (2) H atoms in contact with a plane, 15.35 Å^2; for C_2H_6, (3) H atoms in contact with a plane, *z* perpendicular to plane, 19.32 Å^2. See the text and ref 22 for more discussion. [f] There is no literature *a* value for SF_6, so all van der Waals *a* parameters were recalculated[g] from critical constants.[a] A linear least-squares regression was performed on the reported *a* values and those calculated from the critical constants, giving an R^2 value of 0.999. The *a* value for SF_6 was interpolated from the least-squares line. [g] Barrow, G. M. *Physical Chemistry*; McGraw Hill, New York, 1988; p 42.

distribution of pore sizes available in an amorphous solid, process 1 with pores of fixed dimensions, as in zeolites, will correspond to different types of adsorbate wall interactions for different size adsorbates.

The diameter of the HZSM-5 channel does not allow two molecules to occupy positions adjacent to each other spanning the channel diameter, even for molecules as small as N_2. Therefore, a single molecule is expected to adsorb on the channel wall so as to provide the maximum interaction with the surface. As the adsorbates increase in size, interaction with the distant walls of the cylinder is expected to increase, becoming a maximum when the molecular diameter of the probe is that of the cylinder. Increasing adsorptive size not only leads to increased surrounding wall interaction but also parallels increased surface dispersion interaction for the larger, more polarizable molecules. Thus, the process nomenclature, used earlier for carbon, is incomplete because process 1 for a small molecule will involve pores larger than the adsorptive diameter if they are the smallest ones available. The term "process" will continue to designate the order of *K* values, with process 1 corresponding to the pore that fills first. The term "type" will be used to describe the matching of the adsorbate and pore dimensions. A type 1 adsorbate is one in which the molecular dimensions of the adsorbate match the pore. A type 2 adsorbate interacts strongly with one wall and appreciably with the rest of the pore surface, while a type 3 adsorbate interacts strongly with one wall and weakly with the rest of the pore surface or in larger pores with a molecule on the opposite surface.

The difference in the process and type designation is manifested in the thermodynamic data for adsorption. For the smaller adsorbates, N_2 and CH_4, the larger equilibrium constants for process 1 are also manifested in more negative enthalpies than those for process 2. However, for the larger adsorbates, SF_6 and propane, whose dimensions approach those of the channels, the larger *K* values, at the temperatures studied, correspond to the processes with the less negative enthalpies. Stronger adsorptive−solid interactions will give rise to more negative enthalpies attributed to the smaller pores. However, the equilibrium constants contain entropic contributions,[5] and more negative entropy values in the smaller pores can cause the equilibrium constants for stronger adsorption processes to be smaller than those for weaker adsorption processes.

Adsorption of CO was best defined by a three-process interpretation of the adsorption data. Process 1 is attributed to weak hydrogen bonding with the acid sites of HZSM-5, vide infra. Comparison of the process 2 and 3 enthalpies for CO with 1 and 2, respectively, for N_2 indicates that similar nonspecific interactions are involved.

A plot of the enthalpy of adsorption vs the entropy gives a poor correlation when data for all the processes are combined. Except for methane, the larger $-\Delta H$ process for each adsorptive has a larger $-\Delta S$ value. This is the expected trend except that the increases in $-\Delta S$ for the more negative enthalpy processes are too large to fall on the same line as those for the smaller enthalpy processes. When the data are divided into two different sets of large and small enthalpies for each adsorptive, better correlations are found for each set, Figure 4. The following adsorptives, with the process listed in parentheses, are assigned to the larger $-\Delta H$ line: N_2(1), CO(2), CH_4(1), C_3H_8(2), SF_6(2). The following are assigned to the smaller $-\Delta H$ line: N_2(2), CO(3), CH_4(2), SF_6(1), and C_3H_8(1). The *K* values for the two processes for ethane are too close to resolve, so the data fit to a single process. When ethane is fit to two processes, the process 1 capacity is the same as in the one-process fit. Process 2 is not distinguished from 1, and large errors result in the meaningless process 2 parameters. Thus, least-squares lines are constructed for these two assignments with ethane omitted and shown in Figure 4. The larger $-\Delta H$ plot gives an excellent correlation ($R^2 = 0.90$) even though the type of interaction changes as the adsorbate size increases on going from N_2 and CO to SF_6 and propane. Thus, the slope of the line contains an enthalpy and entropy component from the dispersion interaction to the bound surface and from changing the type of interaction with the remaining surface. Those processes assigned to the smaller $-\Delta H$ line span a range of only four entropy units and as a result give an enthalpy−entropy correlation with small deviations but a poor R^2. The main conclusion from this analysis is the existence of two different enthalpy−entropy plots which indicates two different fundamental groupings of processes. A larger $-\Delta H$ and lower equilibrium constant for the second process is a result of the more negative entropy associated with adsorption of propane and SF_6 in the small channel. With this assignment, process 2 occurs in the small channel, and propane as well as SF_6 is well behaved in the enthalpy−entropy plots. The more exothermic process 1 for methane corresponds to the smaller $-\Delta S$ so the enthalpy criterion would assign this process to the small channel while the entropy criterion would assign this process to the large channel. Also note that the difference in the enthalpies for the two processes is not very large. The single-process fit of ethane gives an average enthalpy value that falls below the large $-\Delta H$ plot.

Table 3. Equilibrium Constants[a,b] and Total Volume Adsorbed at Lowest Temperature[c]

temp[c] (°C)	K_1	K_2	K_3
	HZSM-5/N_2		
−93 (2.4 mmol)	22.7 ± 0.3	2.26 ± 0.34	
−43	1.51 ± 0.01	0.214 ± 0.009	
0	0.260 ± 0.002	0.084 ± 0.002	
25	0.0973 ± 0.0004	0.0791 ± 0.0005	
	HZSM-5/CO		
−93 (2.55 mmol)	414 ± 6	28 ± 3	2.4 ± 3.2
−42	8.69 ± 0.67	1.48 ± 0.33	0.21 ± 0.38
−16	2.56 ± 0.07	0.454 ± 0.036	0.149 ± 0.041
0	1.230 ± 0.004	0.182 ± 0.002	0.147 ± 0.003
	HZSM-5/CH_4		
−84 (2.75 mmol)	85.8 ± 3.0	5.0 ± 6.7	
−42	8.14 ± 0.03	0.548 ± 0.066	
−16	2.309 ± 0.008	0.191 ± 0.018	
0	1.279 ± 0.013	0.126 ± 0.028	
	HZSM-5/C_2H_6		
40(1.78 mmol)	9.504 ± 0.037		
50	5.221 ± 0.020		
75	2.544 ± 0.022		
	HZSM-5/C_3H_8		
125(1.11 mmol)	7.769 ± 0.083	1.760 ± 0.042	
150	5.018 ± 0.021	0.881 ± 0.011	
175	2.199 ± 0.029	0.322 ± 0.014	
	HZSM-5/SF_6		
50 (1.46 mmol)	34.1 ± 0.2	2.94 ± 0.09	
65	19.56 ± 0.09	1.52 ± 0.04	
80	12.57 ± 0.06	0.835 ± 0.029	
	HZSM-5/DME		
150 (1.48 mmol)	11546 ± 9.5	79 ± 37	1.5 ± 4.4
175	3731 ± 2.0	32.7 ± 8.0	0.83 ± 0.92
200	713 ± 1.6	11.8 ± 6.4	0.39 ± 0.74
	FSG/N_2		
−93 (0.74 mmol)	4.9 ± 0.4	0.29 ± 0.03	
−62	0.9 ± 0.4	0.09 ± 0.03	
−44	0.5 ± 0.2	0.05 ± 0.01	
−17	0.14 ± 0.09	0.028 ± 0.007	
	FSG/CO		
−93 (1.24 mmol)	7 ± 1	0.6 ± 0.2	
−62	1.4 ± 0.3	0.14 ± 0.05	
−44	0.7 ± 0.1	0.06 ± 0.02	
−17	0.23 ± 0.09	0.03 ± 0.02	
	FSG/CH_4		
−93 (1.45 mmol)	20 ± 2	0.6 ± 0.2	
−62	2.8 ± 0.3	0.16 ± 0.03	
−44	1.3 ± 0.3	0.09 ± 0.03	
−17	0.4 ± 0.2	0.04 ± 0.02	
	FSG/C_2H_6		
40 (0.308 mmol)	0.6 ± 0.3	0.08 ± 0.04	
55	0.5 ± 0.2	0.05 ± 0.02	
75	0.3 ± 0.1	0.03 ± 0.01	
100	0.19 ± 0.07	0.018 ± 0.008	
	FSG/C_3H_8		
75 (0.35 mmol)	2.9 ± 0.5	0.09 ± 0.02	
125	1.0 ± 0.5	0.03 ± 0.02	
150	0.9 ± 0.2	0.016 ± 0.009	

[a] Gas−solid equilibrium constant (atm^{-1}). [b] The first digit of the uncertainty is the last significant figure. [c] Total experimental amount adsorbed (mmol) at the lowest temperature analyzed is indicated in parentheses.

Dimethyl ether was not included in these correlations because large, specific hydrogen bonding interactions are involved in processes 1 and 2. For specific interactions, the process designations depend on the strength of different groupings of specific donor−acceptor sites. The more negative enthalpies of processes 1 and 2 are consistent with a specific hydrogen bonding interaction. These conclusions will be discussed in more detail in the section on donor probes.

The cause of the two different enthalpy groupings for the processes is attributed to adsorption in the two different size channels of HZSM-5. The more negative enthalpy processes would be assigned to the smaller channels and the less negative enthalpy to the larger channels. Only a difference of 0.2 eu would result from confining an adsorbate in the smaller of the two volumes ($-R \ln (\upsilon_{small}/\upsilon_{large})$). Thus, the entropy differences for the two groupings could result from differing interactions

Table 4. MEA Accessible Surface Areas ($m^2\ g^{-1}$) and Volumes ($mL\ g^{-1}$)[a–c]

	ZSM-5								
	N_2			CO			DME		
process	mmol ads	mL ads	area	mmol ads	mL ads	area	mmol ads	mL ads	area
n_1	1.540 ± 0.015	0.039	141.6	0.612 ± 0.028	0.0173	58.1	0.582 ± 0.005	0.033	91.7
n_2	1.29 ± 0.12	0.032	118.6	1.22 ± 0.17	0.035	115.9	0.147 ± 0.067	0.007	23.2
n_3				1.08 ± 1.3	0.031	102.6	1.2 ± 2.7	0.068	189.1
total	2.83 ± 0.14	0.071	260.2	2.9 ± 1.5	0.083	276.6	1.98 ± 2.8	0.109	303.9
	ZSM-5								
	CH_4			C_2H_6			C_3H_8		
process	mmol ads	mL ads	area	mmol ads	mL ads	area	mmol ads	mL ads	area
n_1	1.994 ± 0.044	0.0593	195.3	1.918 ± 0.016	0.091	277.3	0.514 ± 0.006	0.033	87.5
n_2	0.92 ± 0.68	0.0274	90.1				1.02 ± 0.03	0.066	173.6
total	2.91 ± 0.72	0.0867	285.4	1.92 ± 0.02	0.091	277.3	1.53 ± 0.04	0.099	261.1
	ZSM5			FSG					
	SF_6			N_2			CO		
process	mmol ads	mL ads	area	mmol ads	mL ads	area	mmol ads	mL ads	area
n_1	0.556 ± 0.004	0.043	104.4	0.213 ± 0.001	0.0053	19.6	0.451 ± 0.002	0.0128	42.8
n_2	1.230 ± 0.039	0.095	231.0	2.48 ± 0.07	0.0620	228.1	2.2 ± 0.1	0.062	209.0
total	1.790 ± 0.043	0.138	335.4	2.69 ± 0.07	0.0674	247.7	2.6 ± 0.1	0.075	251.8
	FSG								
	CH_4			C_2H_6			C_3H_8		
process	mmol ads	mL ads	area	mmol ads	mL ads	area	mmol ads	mL ads	area
n_1	0.330 ± 0.001	0.0098	32.3	0.284 ± 0.002	0.007	41.1	0.111 ± 0.0001	0.013	18.9
n_2	3.03 ± 0.14	0.0901	296.7	2.3 ± 0.2	0.18	332.6	2.8 ± 0.2	0.11	476.7
total	3.3 ± 0.1	0.0999	329.0	2.6 ± 0.2	0.19	373.6	2.9 ± 0.2	0.12	495.6

[a] Surface areas in $m^2\ g^{-1}$; process volumes in $mL\ g^{-1}$. [b] For molecular surface areas and volumes, see Table 2. [c] The first digit of the uncertainty is the last significant figure.

Table 5. Enthalpies and Entropies[a]

		$-\Delta H_{1,2,3}$ (kcal/mol)	$-\Delta S_{1,2,3}$ ((cal/deg)/mol)
N_2	A572	4.5 ± 0.2, 4.1 ± 0.2, 3.1 ± 0.1	17.8 ± 0.3, 19.6 ± 0.8, 17.1 ± 0.7
	HZSM5	4.9 ± 0.2, 3.2 ± 0.4	20 ± 1, 16 ± 2
	FSG	4.2 ± 0.4, 2.9 ± 0.1	20 ± 1, 18.4 ± 0.3
CO	A572	5.2 ± 0.1, 4.7 ± 0.3, 3.0 ± 0.2	18 ± 1, 18 ± 1, 19 ± 1
	HZSM5	6.11 ± 0.09, 5.2 ± 0.3, 3.1 ± 0.5	22.0 ± 0.4, 22 ± 1, 16 ± 2
	FSG	4.1 ± 0.2, 3.6 ± 0.2	18.7 ± 0.7, 21.05 ± 0.72
CH_4	A572	6.6 ± 0.5, 5.6 ± 0.1, 4.4 ± 0.1	20 ± 2, 20.2 ± 0.9, 19 ± 1
	HZSM5	5.1 ± 0.1, 4.54 ± 0.09	18.3 ± 0.5, 20.9 ± 0.4
	FSG	4.6 ± 0.1, 3.2 ± 0.1	19.5 ± 0.3, 18.9 ± 0.6
C_2H_6	A572	9.0 ± 0.2, 7.7 ± 0.1, 6.7 ± 0.1	21 ± 1, 20.01 ± 0.82, 20.9 ± 0.9
	HZSM5	8.159 ± 0.001	21.580 ± 0.004
	FSG	5.0 ± 0.4, 5.6 ± 0.3	16 ± 1, 22.4 ± 0.8
C_3H_8	A572	10 ± 0.2, 9.1 ± 0.1, 8.6 ± 0.8	20.2 ± 10.2, 18.6 ± 1.1, 20.5 ± 1.1
	HZSM5	9 ± 2, 12 ± 2	18 ± 5, 29 ± 4
	FSG	4.9 ± 0.8, 6.8 ± 0.8	12 ± 2, 24 ± 1
SF_6	A572	8.6 ± 0.7, 7.0 ± 0.3, 6.6 ± 1.2	16.4 ± 2, 16.2 ± 0.9, 19.6 ± 3.6
	HZSM5	7.5 ± 0.3, 9.52 ± 0.02	16.4 ± 0.9, 27.32 ± 0.07
DME	HZSM5	22 ± 3, 15 ± 1, 10 ± 1	33 ± 7, 27 ± 3, 24 ± 3

[a] The first digit of the uncertainty is the last significant figure.

with the distant wall and from more efficient packing of the adsorbate molecules for the more negative enthalpy process.

Figure 5 is a plot of the entropies of adsorption versus the entropies of vaporization of the liquids. The entropy for the small channel is more negative than the entropy of vaporization as expected for a more confined molecule. The increase in entropy for the larger molecules also has the contributions normally observed[20] from a more negative enthalpy of interaction. The entropies for the larger channel are less negative than the entropies of vaporization and indicate a weaker constraint in this channel than in the liquid. The errors are larger than those of the small channel, and the slope of the line is 0.3 ± 0.6. In addition, more ordering of the hydroxyl functionality or a greater loss of vibrational freedom for the silicon and aluminum atoms comprising the walls of the small channels than that for the large channel could lead to a more negative entropy for the small channel when adsorption occurs. Calorimetric analysis[21] of the acidity of HZSM-5 has shown that the small channel contains most of the hydroxyl functionality. These different entropy components for the two channels lead to the two different enthalpy−entropy plots.

(20) Person, W. B. *J. Am. Chem. Soc.* **1976**, *84*, 536.

(21) Drago, R. S.; Dias, S.; Torrealba, M.; de Lima, L. *J. Am. Chem. Soc.* **1997**, *119*, 4444−4452.

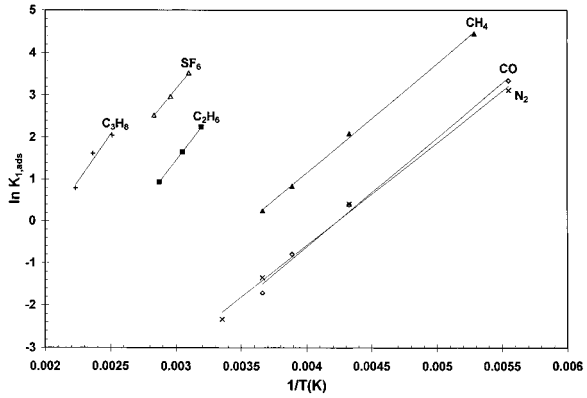

Figure 3. ln K_1 vs $1/T(K)$ plots for various adsorptives by HZSM-5.

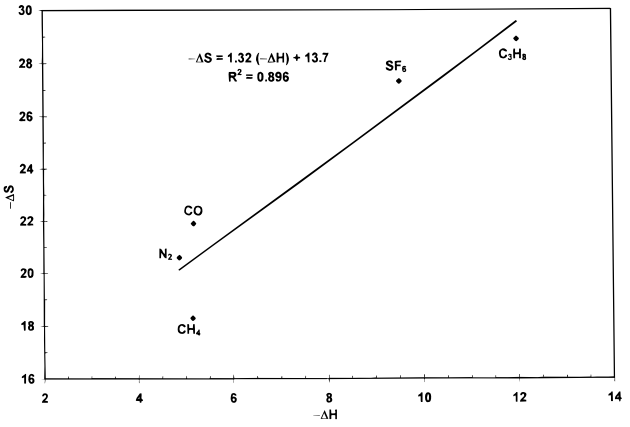

Figure 4. $-\Delta S_{\text{small pore}}$ vs $-\Delta H_{\text{small pore}}$ for HZSM-5. The gases are labeled.

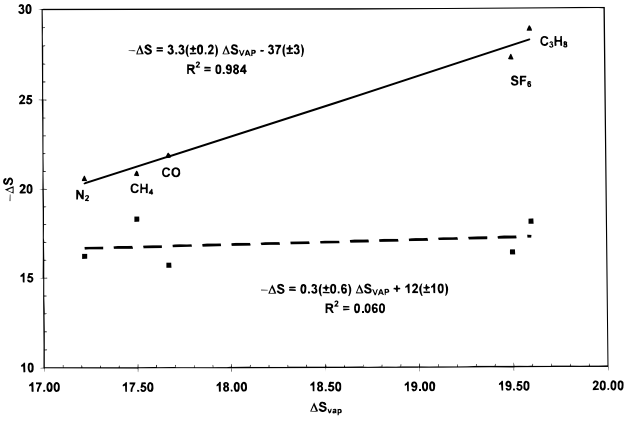

Figure 5. Entropy of adsorption vs the entropy of vaporization. The solid line is for the small pores, and the dashed line is for the large pores.

The reversals in equilibrium constants and enthalpies observed in HZSM-5 are not observed in the carbon adsorbents studied to date. This is attributed to slit-shaped pores in carbon in contrast to those in HZSM-5 and other zeolites whose channels approximate cylinders. The slit-shaped pores lead to less molecular reorganization when a large molecule is adsorbed. Low-energy bending of the O−Si−O angles also leads to some flexibility in the channel dimensions of a zeolite which can lead to entropy contributions. Carbon entropies do not exceed −21 (cal/mol)/deg for the adsorptives studied here.

Further insights concerning adsorbent−adsorbate interactions arise from plots of the enthalpies vs the square root of the van der Waals *a* parameter. Figure 6 shows a good correlation (R^2 = 0.95) of the more negative enthalpy processes, and a better correlation ($R^2 = 0.99$) of the less negative enthalpy plots. Linear van der Waals plots ($R^2 = 0.99$)[4] for carbon adsorbents assumed that the type of interaction is the same for a given process for all molecules. The adsorptive selects pores from the distribution available to undergo similar adsorbate−wall interactions for all molecules involved in the *i*th processes. For the fixed channel dimensions of HZSM-5, the slopes of the lines in Figure 5 have an additional contribution to these plots from a change in the type of interaction as the adsorbate size increases.

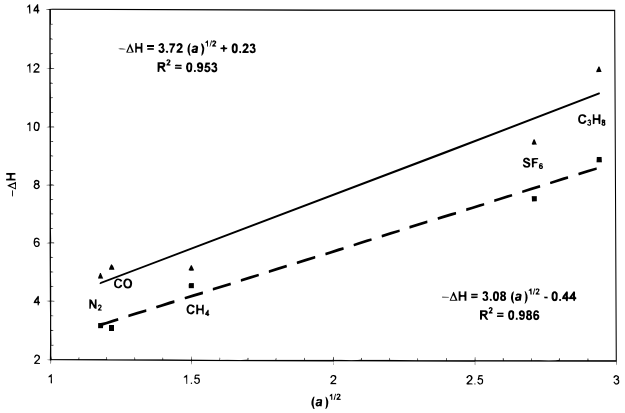

Figure 6. Enthalpy of adsorption vs van der Waals $a^{1/2}$ for the small pores (solid line) and large pores (dashed line) of HZSM-5.

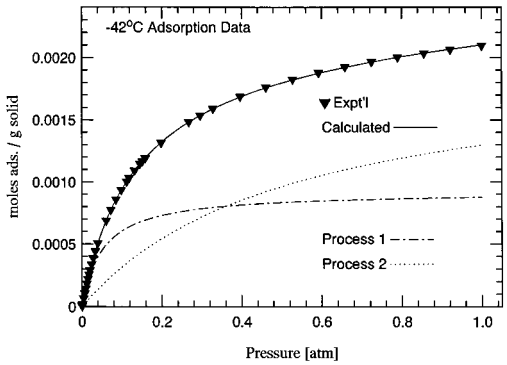

Figure 7. Process-resolved isotherms for CH_4 adsorption by HZSM-5 calculated from the MEA *n* and *K* values.

For ethane, the van der Waals plot indicates that the single-process enthalpy for ethane is less negative than expected for the more negative enthalpy processes and more negative than expected from the smaller $-\Delta H$ plot. This behavior is expected if the MEA provides an average enthalpy because the two *K* values cannot be resolved.

Insights from the Process Capacities. As shown above, the multiple-equilibrium thermodynamic parameters provide unprecedented detail about the adsorption process. Even more detail results from the MEA capacities of the processes, $n_{i,\text{ads}}$. The capacities in moles and the equilibrium constants, $K_{i,\text{ads}}$, can be substituted into eq 3 to resolve the total isotherm into the process 1 and 2 components. This resolution is shown in Figure 7 for CH_4 with HZSM-5 and shows that, at all measured pressures, adsorption occurs simultaneously in both channels of the solid during the adsorption process.

The process capacities (mmol g^{-1}) (Table 4) decrease as the size of the gas molecules increases (Table 2). These capacities can be converted into the surface areas and pore volumes for the individual processes using the molecular areas and molar volumes of the adsorbates, respectively. Different literature reports give adsorbate molar volumes and areas that vary

considerably. Accordingly, these quantities were calculated using ZINDO,[22] and the calculated values are given in Table 2. The calculated surface areas are based on the projected areas for orientations of the molecules that are expected to provide the maximum dispersion interaction with the surface of the solid. June *et al.*[11] report that the channels of the zeolite exhibit constraining effects upon long hydrocarbon chains, such that these molecules are forced to take on a more elongated shape. The orientations employed are given in the Table 2 footnotes. The calculated total MEA accessible surface areas reported in Table 4 for HZSM-5 are (N_2) 260 $m^2\ g^{-1}$, (CO) 277 $m^2\ g^{-1}$, (CH_4) 285 $m^2\ g^{-1}$, (C_2H_6) 278 $m^2\ g^{-1}$, (C_3H_8) 261 $m^2\ g^{-1}$, and (SF_6) 335 $m^2\ g^{-1}$. For nitrogen, the milliliters of gas adsorbed in the two processes is low compared to other adsorbates, indicating that the N_2 molecules are not packed as closely to each other as they are in the liquid or that gaps exist in the extent of surface coverage near the channel intersections where 9 Å diameter voids exist.[11] The bond axis of CO is expected to be linear to the O−H bond for the specific interaction of process 1. CO is expected to adsorb parallel to the surface for the nonspecific dispersion interaction of processes 2 and 3. The area for CO, calculated assuming that the n_1 process is C bonded perpendicular to the surface and physisorption is parallel results in an area of 260 $m^2\ g^{-1}$. If the O−H bond is not perpendicular to the surface, a value approaching 277 $m^2\ g^{-1}$ results. The propane molecule is assumed to have two hydrogens from each methyl and one from the methylene interacting with the surface. The more polarizable SF_6 has a stronger surface interaction and results in more effective coverage in the channels and into the intersections. Thus, surface area is adsorptive dependent, and for small molecular weight gases above the critical temperature a value around 275 $m^2\ g^{-1}$ results.

In all instances, the process capacities for the small channels are greater than those of the large channel. This is consistent with the small channels having a zigzag shape and the large ones being straight.

Ethane has dimensions that could permit it to span the diameter of the channel with the C−C bond perpendicular to the surface. In this orientation, ethane would have two sets of three hydrogens interacting with the solid surface of opposite walls. The molecular surface area per wall for ethane in this configuration is 19.32 $Å^2$, as calculated by ZINDO. If ethane lies flat, an eclipsed conformation, with four hydrogens interacting with the surface, is expected. The molecular surface area for ethane in this configuration is 24.01 $Å^2$. The calculated MEA surface area for ethane adsorbing parallel is 278 $m^2\ g^{-1}$, and 223 $m^2\ g^{-1}$ for ethane perpendicular to the surface in both channels. These considerations suggest that ethane is adsorbed with its bond axis parallel to the surface and illustrates the unparalleled, detailed insight available about adsorption from MEA.

Pore volumes from MEA can be compared to the micropore pore volume measured with the H−J *t*-plot for HZSM-5 at 77 K which was found to be 0.14 mL g^{-1}. Calculation of the total pore volume by MEA (Table 4) for N_2 indicates a total volume of 0.07 mL g^{-1} consistent with its low surface area. Adsorption on the surface of the 9 Å voids at liquid nitrogen temperatures normally used for N_2 porosimetry measurements could give rise to a third, lower enthalpy process which accounts for the large volume from porosimetry. The equilibrium constant for this third process is too low to contribute above the critical temperature and at the pressures employed for the N_2 isotherms in this study.

(22) Drago, R. S.; Webster, C. E. Submitted for publication.

The larger adsorbates give larger values for the accessible pore volume. Adsorption of SF_6 resulted in an MEA volume of 0.14 mL g^{-1} which is comparable to that from the *t*-plots. The other adsorbates give MEA volumes of 0.09 ± 0.01 mL g^{-1}. When the surface of a pore is completely covered by adsorbates of smaller dimensions than the channel, the area from the adsorbate to the distant wall is empty space that is not calculated as pore volume. This empty space accounts for part of the lower volumes found for the other adsorbates than that found for SF_6. The most accurate assessment of the structural channel volume of the solid comes from adsorbates whose dimensions match that of the pore and which pack efficiently. When this is not the case, the adsorbent capacity is a utilized pore volume that is adsorptive dependent. At lower temperatures condensable adsorptives are expected to reveal an additional process corresponding to adsorption on the surface of the channel intersections. The important point is that the structural pore volume of the solid is not as relevant a quantity for understanding adsorption as is the pore volume utilized by the particular adsorptive employed at the conditions of the experiment. Clearly, this detailed understanding of adsorption provided by MEA is relevant for interpreting results from applications of zeolites in gas separation or gas phase catalysis when carried out above the critical temperature of the gas.

For methane, the process capacities support the enthalpy conclusion and indicate that process 1 occurs in the smaller channel. However, the more negative methane enthalpy is comparable to that of N_2, falls on the enthalpy−entropy plot, but is low on the van der Waals plot. One possibility for a lower than expected enthalpy would involve interaction of the edge instead of the face of the tetrahedral methane molecule with the solid surface in the small channel. Interaction for this configuration would be mainly driven by entropy considerations with some stabilization from opposite wall interactions. Leaving methane out of the more negative enthalpy−entropy plot (Figure 4) gives the equation $-\Delta S_{small} = 1.15(-\Delta H) + 15.6$ and improves the R^2 to 0.97 from 0.90. The surface areas for methane packed in the manner proposed above is 269 compared to 285 $m^2\ g^{-1}$ for adsorption with the 3-fold axis perpendicular to the surface. Thus, areas do not distinguish the adsorption mode. The process 2 enthalpy is well behaved in the van der Waals plot, suggesting that methane packs in the large channel with its 3-fold axis perpendicular to the surface.

Interpretation of the Process Groupings for Donor Probes. In an earlier report from this laboratory,[21] it was shown that titration of HZSM-5 slurried in cyclohexane with pyridine revealed 0.042 mmol of a very strong acid site and 0.53 mmol g^{-1} of hydrogen bonding sites. Titrations with 2,6-lutidine and 2,6-di-*tert*-butylpyridine indicate that the strong sites were located in the small channels, 0.32 mmol of hydrogen bond sites were located in the small channel, 0.18 mmol g^{-1} of hydrogen bond sites were located in the large channels, and 0.034 mmol were located on the exterior surface. It was also shown that when the solid was studied at elevated temperatures the strong and weak acid sites could not be resolved because the equilibrium constants approached one another. These conclusions are consistent with the dimethyl ether results from MEA. At the temperatures employed the strong acid n_1 sites are not distinguished from the weaker n_2 sites found by cal-ad for pyridine, and an n_1 value of 0.58 mmol g^{-1} results for $(CH_3)_2O$. The van der Waals plot suggests that about 11 kcal mol^{-1} of the process 1 enthalpy for $(CH_3)_2O$ arises from the nonspecific component of the gas−solid interaction and 11 kcal mol^{-1} from the average specific donor−acceptor interaction of the strong

and weaker acid sites found in the pyridine titration. Process 2 has a 7 kcal mol^{-1} more negative enthalpy than expected from the nonspecific interaction estimated from the van der Waals plot.

Comparison of n_1 for CO with n_1 for DME indicates that both gases are involved in a specific interaction with the same number of hydrogen bonding sites. CO is weakly basic compared to DME, and this is reflected in the magnitude of the enthalpies for the first process. The 0.6 mmol g^{-1} capacity is the same as that for process 1 for $(CH_3)_2O$. This indicates that the density of acid sites is such that they are accessed by both molecules. This result occurs even though the surface area required to accommodate site 1 for $(CH_3)_2O$ is twice that of CO. The process 2 capacity in mmol g^{-1} for dimethyl ether compared to lutidine suggests that the weak hydrogen bond sites in the large channel are included in the process 2 capacities. Such a conclusion is also suggested by the deviation of 7 kcal mol^{-1} of process 2 for $(CH_3)_2O$ from the process 1 van der Waals plot.

With only specific interactions measured for the pyridine titration in hexane, the pore volumes required are 0.032 mL g^{-1} for the small pore and 0.012 mL g^{-1} for the large pore. Hexane fills the rest of the pore volume.

The bulk silica/alumina ratio of 53 corresponds to a Si/Al atom ratio of 23.5 which is used to calculate the millimoles of aluminum per gram of HZSM-5. The ~0.6 mmol of n_1 acid sites of HZSM-5 from the MEA of CO and $(CH_3)_2O$ correspond to 0.58 mmol g^{-1} of aluminum atoms giving rise to Si−O(H)−Al sites.

Adsorption by Silica Gel. Adsorption isotherms on Fisher silica gel, FSG, for nonspecific adsorbates, are also best fit by a two-process analysis of the adsorption data. This is a significant result because the pores in FSG are not expected to be as homogeneous in size or shape as the channels of HZSM-5. Process 1 enthalpies for N_2, CO, and CH_4 on FSG are less negative than those for the small channel of HZSM-5 and comparable to the large channel enthalpies for HZSM-5, Table 5. This suggests that the small pores of silica gel are of comparable size to those of the large channel of HZSM-5. The more negative enthalpy, propane process (process 2) on FSG is also within experimental error of that for the large channel of HZSM-5. The capacities, Table 4, indicate that the volume of the FSG small pores is very low, about 0.01 mL g^{-1}. It is noteworthy that *t*-plots detect a small micropore capacity of 0.02 mL g^{-1}. Most of the adsorption capacity of FSG arises from larger pores. Comparison of the FSG less negative enthalpies with those for the larger channels of HZSM-5 indicate that these involve slightly larger channels in FSG which are not in the mesopore regime. The *t*-plots indicate 0.33 mL g^{-1} of mesopores. MEA indicates 0.10 mL g^{-1} for process 2 capacities which increase to 0.19 for propane. Apparently these large micropores are included in the mesopores of the *t*-plot analysis. The remaining 0.14 mL g^{-1} of mesopores from the *t*-plot analysis are not accessed by any process for the adsorbates studied at these temperatures and pressures. Lower temperatures or higher pressures are needed to populate the weaker energy adsorption process that occurs in the mesopores. This emphasizes that porosity must be determined under conditions relevant to the application. For any applications involving gases similar to those studied, porosity that is not accessed is not relevant.

Since the bulk compositions of FSG and HZSM-5 are similar, the differences in the MEA results dramatically illustrate the influences of porosity on adsorption. One major difference in the reactivity of HZSM-5 and FSG is the strong acidity of the former. The two-process fit of CO with enthalpies that fit the van der Waals plot indicate the absence of acid sites strong enough to undergo a specific interaction with silica gel.

Reversals in process enthalpies and equilibrium constants are observed for propane with silica gel. Consistent with this, process 2 for propane falls on the small pore van der Waals plot for other substrates and process 1 for propane falls on the large pore plot.

$$-\Delta H_1 = 1.458(\pm 0.098)a^{1/2} + 2.381(\pm 0.19) \quad R^2 = 0.987 \tag{4}$$

$$-\Delta H_2 = 1.138(\pm 0.30)a^{1/2} + 1.829(\pm 0.60) \quad R^2 = 0.824 \tag{5}$$

The enthalpy−entropy plots and the entropy of adsorption−entropy of vaporization plots show the same behavior as in the case of HZSM-5 for the small pore data. The large pore data are poorly behaved in both plots. This suggests that the pores involved in the large pore processes involve a different distribution of pore sizes for N_2 and CO compared to ethane and propane.

The BET surface area of silica is reported to be 508 m^2 g^{-1}. The MEA results show a decided adsorptive dependence of the surface area. For example, methane gives an area of 329 m^2 g^{-1}, and the total area for propane is 496 m^2 g^{-1} with 478 m^2 g^{-1} arising from the more negative enthalpy process. This is attributed to a better matching of the pore distribution to the propane dimensions.

Effective Pressure. In heterogeneous catalysis, porosity in supports enhances adsorption and concentrates reactants around catalytic sites, thereby increasing the reaction rate. The concept of effective pressure, P_{eff}, was introduced[4a] as a way to compare the concentrating power of solid supports. Effective pressure is the pressure that would have to be applied to an ideal gas to obtain a concentration in the gas phase equal to the moles of gas adsorbed per milliliter of pore volume in the support. The moles of gas adsorbed by different adsorbents varies with the pressure of gas over the solid and the temperature. P_{eff} is defined at 25 °C so the number of moles adsorbed, $n_{ad,1atm}$ is calculated from the MEA *K* and *n* values at this temperature. Using the ideal gas law, the number of moles adsorbed is converted to P_{eff} using the total MEA volume, $\sum n_i$ (mL/g) in eq 6. P_{eff} indicates that 194 atm would be required to match

$$P_{eff} = \frac{n_{ad,1atm}RT}{\sum n_i \text{ (mL/g)}} \tag{6}$$

the effective pressure of methane in HZSM-5. This compares to 98 atm for the carbonaceous adsorbent A572, and a P_{eff} of 21 atm for silica gel. Thus, porosity permits one to carry out a reaction in the pores of HZSM-5 at 1 atm of external pressure which requires 200 atm of CH_4 in the gas phase.

Conclusions

Adsorption isotherms for seven adsorptives were measured at multiple temperatures above their critical temperatures with a zeolite, HZSM-5, and silica gel. The MEA, which fits the isotherms simultaneously to a minimum number of processes, provides enthalpies, entropies, and process capacities. In amorphous adsorbents the processes contain a distribution of pore dimensions. If this distribution is narrow enough to give the same thermodynamic interaction parameters within experimental error, it is reasonable to group them together in describing the adsorption process. HZSM-5 was selected for

study because it contains two channels with slightly different, fixed dimensions. The adsorption data for HZSM-5 are fit with the MEA model using two adsorption processes, providing a check on the meaning of the model. Examination of a solid with fixed dimensions has provided not only a test of the applicability of the MEA model but also insights into the very complex energetics of adsorbate−adsorbent interactions. Unlike amorphous adsorbents, where an adsorptive can select pores of similar size from the distribution available for process 1, the first adsorption process that occurs in materials with uniform, fixed dimensions may not involve a pore of comparable size. Since the process designations for different size adsorbates correspond to different interaction potentials, a type designation is used to indicate the matching of adsorptive and pore dimensions. The correlations of enthalpies of adsorption to entropies and van der Waals constants reveal a specific interaction giving rise to one process for CO and two for dimethyl ether.

Reversals in the magnitude of the enthalpy and equilibrium constant are found for the processes corresponding to adsorption of propane and SF_6 by HZSM-5. Process 1 has the larger K and less negative enthalpy, indicating a type 2 interaction. A wide variety of probe molecules have been studied on carbonaceous adsorbents, and none show this reversal. In contrast to HZSM-5, the pores of the carbonaceous A-572 consist of parallel sheets or planes with localized graphitic domains. The adsorbate−adsorbent interactions occur along the surfaces of these planes, and a large adsorbate is less constrained in a slit than it is in a cylinder. Reversals in K and ΔH can be expected in cylindrical-shaped pores.

The process capacities that result from the MEA are as significant as the thermodynamic data. Using molar volumes, one can calculate the accessible pore volume for an adsorbate. When adsorptive dimensions match pore dimensions, structural pore volumes result. Comparison of these volumes with those from standard N_2 porosimetry show important differences. For measurements above the adsorptive critical temperature, monolayer coverage is expected and conversion of the process capacities from MEA to molecular areas provides accessible surface areas. Significant differences result between the values obtained in this manner and those from BET on microporous solids.

The larger equilibrium constants obtained for HZSM-5 compared to silica gel indicate that the zeolite has a larger affinity for adsorbing these molecules as a result of the presence of smaller, defined channel dimensions with larger capacities. The credibility of the MEA model is enhanced by its ability to provide a rational explanation of adsorbent differences using thermodynamic and capacity criteria. Clearly much more useful information is obtained from an MEA characterization than other isotherm analyses.

Acknowledgment. This work was supported by the US Army ERDEC and ARO. The authors thank Micromeritics Instrument Corp. for their assistance and technical support.

JA972466W